Rhodopsin-mediated light-off-induced protein kinase A activation in mouse rod photoreceptor cells

Shinya Sato[a,1], Takahiro Yamashita[b], and Michiyuki Matsuda[a,c]

[a]Laboratory of Bioimaging and Cell Signaling, Graduate School of Biostudies, Kyoto University, 606-8501 Kyoto, Japan; [b]Department of Biophysics, Graduate School of Science, Kyoto University, 606-8502 Kyoto, Japan; and [c]Department of Pathology and Biology of Diseases, Graduate School of Medicine, Kyoto University, 606-8501 Kyoto, Japan

Edited by King-Wai Yau, Johns Hopkins University School of Medicine, Baltimore, MD, and approved September 9, 2020 (received for review May 8, 2020)

Light-induced extrasynaptic dopamine release in the retina reduces adenosine 3′,5′-cyclic monophosphate (cAMP) in rod photoreceptor cells, which is thought to mediate light-dependent desensitization. However, the fine time course of the cAMP dynamics in rods remains elusive due to technical difficulty. Here, we visualized the spatiotemporal regulation of cAMP-dependent protein kinase (PKA) in mouse rods by two-photon live imaging of retinal explants of PKAchu mice, which express a fluorescent biosensor for PKA. Unexpectedly, in addition to the light-on-induced suppression, we observed prominent light-off-induced PKA activation. This activation required photopic light intensity and was confined to the illuminated rods. The estimated maximum spectral sensitivity of 489 nm and loss of the light-off-induced PKA activation in rod-transducin-knockout retinas strongly suggest the involvement of rhodopsin. In support of this notion, rhodopsin-deficient retinal explants showed only the light-on-induced PKA suppression. Taken together, these results suggest that, upon photopic light stimulation, rhodopsin and dopamine signals are integrated to shape the light-off-induced cAMP production and following PKA activation. This may support the dark adaptation of rods.

retina | two-photon microscopy | FRET biosensor | protein kinase A | rhodopsin

Vertebrate photoreceptor cells, i.e., rods and cones, convert light information into electrical signals through an enzymatic process called phototransduction (1–4). In this process, light-activated visual pigments, rhodopsin in rods, and cone visual pigments in cones activate heterotrimeric G protein transducin and thereby phosphodiesterase, culminating in the degradation of cyclic guanosine-3′,5′-monophosphate (cGMP). The reduction in cGMP concentration causes closure of cGMP-dependent channels in the plasma membrane to evoke an electrical response. For the timely update of visual information, activated visual pigments and their downstream enzymes are, then, rapidly deactivated (5) and when back in darkness, the cGMP level is restored by guanylate cyclase (GC) (6, 7).

Ca^{2+} is the primary factor that decelerates the shut off processes of phototransduction and thereby increases photoreceptor sensitivity (7–9). Under scotopic conditions, Ca^{2+} flows into photoreceptor cells through the cGMP-gated cation channel. Ca^{2+} binds to calcium-binding proteins, including S-modulin/recoverin and GC activating proteins (GCAPs). Ca^{2+}-liganded S-modulin/recoverin inhibits rhodopsin phosphorylation through inhibition of G protein coupled receptor kinase 1 (GRK1) to delay the quenching of photoactivated rhodopsin by arrestin (10). On the other hand, Ca^{2+}-liganded GCAPs are negatively modulated and do not activate the cGMP restoration by GC (6). Thereby, high Ca^{2+} in scotopic conditions delays the recovery of the photoresponse and increases the sensitivity of photoreceptor cells (5).

Recently, in addition to Ca^{2+}, cAMP has been suggested to increase photoreceptor sensitivity (11). Similar to the Ca^{2+} level, the cAMP level in photoreceptors is reduced by light via a dopamine-mediated mechanism (12, 13). Dopamine is released extrasynaptically from dopaminergic amacrine cells in a light-dependent manner (14, 15). Photoreceptor cells detect dopamine with the dopamine receptor D4 (D4R) (16, 17), which is coupled with G_i to inhibit adenylate cyclase (AC) and thereby to reduce cAMP (18). A number of previous studies showed that cAMP-dependent protein kinase (PKA) phosphorylates several phototransduction components. PKA phosphorylates GRK1 to reduce its rhodopsin phosphorylation ability (19), regulator of G protein signaling 9–1 to reduce its GTPase activating protein activity (20), phosducin to accelerate the trafficking of transducin toward the outer segment (21), and GC to increase its sensitivity to Ca^{2+}-dependent inhibition (22). These studies suggest a role of PKA in increasing photoreceptor sensitivity. Indeed, Astakhova and colleagues showed that pharmacological activation of the cAMP production induces a twofold increase in the signal-to-noise ratio in frog rods (11, 23). Furthermore, PKA strengthens the electrical coupling of photoreceptor cells via the phosphorylation of connexin36 (24) to increase the visual sensitivity (25). Taken together, these findings strongly suggest that light reduces cAMP levels to desensitize photoreceptor cells via PKA suppression. However, unlike in the case of cGMP regulation, which has been studied electrophysiologically with single-cell resolution and millisecond precision, there are currently no available methods to monitor cAMP in living photoreceptor cells, which limits the systematic characterization of its spatiotemporal regulation in photoreceptors.

Here, we used a two-photon PKA activity imaging method to address this deficiency. A retinal explant culture for imaging was prepared from PKAchu mice (26–28) that ubiquitously express a

Significance

Rod photoreceptor cells mediate scotopic vision using rhodopsin and its downstream signal transduction cascade to degrade guanosine 3′,5′-cyclic monophosphate (cGMP). However, less is known about another rod photoresponse: dopamine-mediated cAMP degradation, which contributes to the visual desensitization. Here, we show the fine time course of rod cAMP regulation using a two-photon microscope and fluorescent protein probe for cAMP-dependent protein kinase (PKA). Unexpectedly, the light-induced PKA suppression was followed by robust PKA activation upon light off. Our data strongly suggest the involvement of rhodopsin in this activation and, thus, the presence of its alternative output toward cAMP. The light-off-induced PKA activation might contribute to an efficient dark adaptation after the transition from light to dark environment.

Author contributions: S.S. and M.M. designed research; S.S. performed research; S.S. and T.Y. analyzed data; and S.S., T.Y., and M.M. wrote the paper.

The authors declare no competing interest.

This article is a PNAS Direct Submission.

[1]To whom correspondence may be addressed. Email: sato.shinya.7e@kyoto-u.ac.jp.

This article contains supporting information online at https://www.pnas.org/lookup/suppl/doi:10.1073/pnas.2009164117/-/DCSupplemental.

First published October 12, 2020.

Förster resonance energy transfer (FRET)-based PKA activity sensor protein, AKAR3EV (29, 30). Unexpectedly, in addition to the aforementioned light-on-induced PKA suppression, we observed a prominent light-off-induced PKA activation in photoreceptor cells. This PKA activation was induced by photopic light stimulation and confined to rod photoreceptor cells in the illuminated area. Spectral sensitivity data suggested the involvement of rhodopsin in the PKA activation. Consistent with this suggestion, the activation was not detected from retinal explants that were deficient in rhodopsin signaling. Interestingly, the rhodopsin-deficient retinas showed only light-on-induced PKA suppression. From these results, we propose that rhodopsin and dopamine signals are integrated to shape the light-off-induced PKA activation in rods.

Results

Ex Vivo Two-Photon Imaging Delineates Various Layers of the PKAchu Mouse Retina. First, we set up two-photon live imaging of the isolated mouse retina (Fig. 1*A*). A retina from a PKAchu mouse was flat mounted on a culture insert. The insert was then placed under a two-photon microscope and perfused with oxygenated culture medium. The PKA biosensor AKAR3EV (*SI Appendix*, Fig. S1*A*) was expressed ubiquitously in PKAchu mice, which allowed us to delineate tissue morphology at the subcellular level in six different layers of the retina (Fig. 1 *B*–*H* and Movie S1). The nuclear-sparing pattern was caused by the cytoplasmic localization of AKAR3EV (30). The outer nuclear layer (ONL) thickness at 1.0 mm superior from the optic nerve head (ONH) was 54.3 ± 2.9 μm (mean ± SD, $n = 12$ retinas), which is comparable to the value for the young-adult wild type (31). Intriguingly, a subset of cells in the photoreceptor layer (Fig. 1 *E*–*H*) expressed AKAR3EV much more abundantly (AKAR3EV^{high} cells) than the rest (AKAR3EV^{low} cells). Therefore, to prevent saturation of the detector, we needed to reduce the excitation laser power from the outer plexiform layer (OPL; arrow in Fig. 1*H*). Please note that this intensity difference does not mean high and low PKA activities. Although PKA increases the FRET efficiency of AKAR3EV (*SI Appendix*, Fig. S1*A*) to induce the spectral shift of the fluorescence, the corresponding intensity change is limited (*SI Appendix*, Fig. S1*B*).

In the OPL, the large size and shape of the AKAR3EV^{high} photoreceptor cells closely resembled the cone pedicles (Fig. 1*E*) (32). Moreover, the nuclei of the AKAR3EV^{high} photoreceptor cells (white arrowheads in Fig. 1*H*) were located near the interface between the ONL and the photoreceptor segments layer (PRS). These observations strongly suggested that the AKAR3EV^{high} and AKAR3EV^{low} cells are cones and rods, respectively. This was confirmed by using rhodamine labeled peanut agglutinin (PNA-rhodamine), which specifically binds to the extracellular sheath of cones (33). As expected, PNA-rhodamine labeled the tips of the AKAR3EV^{high} cells (Fig. 1*I* and Movie S2). In conclusion, our two-photon imaging method clearly delineates the layer structure of the PKAchu retina and enables comparison of PKA activities in rods and cones.

The PKAchu Retina Visualizes Cell-Type-Specific PKA Regulation by Dopamine. To confirm whether AKAR3EV detects PKA activity in the retina, we first examined the response to forskolin, which increases the cAMP level by stimulating AC. The mode of action of AKAR3EV and the method to generate PKA activity images were described previously (34, 35). Briefly, the signal intensity in the FRET-acceptor channel (FRET Ch) was divided by that of FRET-donor channel (CFP Ch) to obtain FRET/CFP-pseudocolor images, which depict PKA activity (*SI Appendix*, Fig. S1*B*). As expected, 20 μM forskolin strongly increased FRET/CFP in all layers of the retina (*SI Appendix*, Fig. S2 *A* and *B* and Movie S3). Interestingly, this elevation was less pronounced in cones (white arrowheads in *SI Appendix*, Fig. S2*A*) than in rods, which may be ascribable to the difference in AC subtypes (36).

Next, we examined the response to dopamine, which is one of the major neurotransmitters that modulates visual processing in the retina (37). Dopamine either activates or inactivates PKA, depending on the type of dopamine receptors: D1-like receptors (D1R and D5R) activate PKA via G_s, whereas D2-like receptors (D2R, D3R, and D4R) suppress PKA via G_i (13). In the mouse retina, D1R is expressed in horizontal cells and a subset of bipolar and amacrine cells in the inner retina (38). On the other hand, D4R is expressed in photoreceptor cells (16, 24). In agreement with this layer-specific distribution, 10 μM dopamine increased FRET/CFP values in the inner plexiform and inner nuclear layers, and decreased them in photoreceptor cells (*SI Appendix*, Fig. S2 *C* and *D* and Movie S4). Therefore, we concluded that AKAR3EV in the PKAchu retina detects both PKA activation and suppression.

Light-Induced PKA Suppression Is Followed by an Unexpected "Overshoot" of Activation in Photoreceptor Cells. According to previous studies, light induces extrasynaptic dopamine release from dopaminergic amacrine cells, which reduces cAMP in photoreceptor cells (16, 39, 40). However, previous studies did not elucidate the fine time course of this response; therefore, we time lapse imaged the light-induced cAMP reduction via PKA activity change. Dark- and light-adapted PKAchu retinas were prepared for imaging (please see *SI Appendix*, *Supplementary Methods* for details about preparations). As expected from previous studies that reported the elevated photoreceptor cAMP level in darkness (40, 41), the basal PKA activity in photoreceptor cells was significantly greater in the dark-adapted retina (Fig. 2 *A* and *B*, PRS). To measure the time course of the photoresponse, a

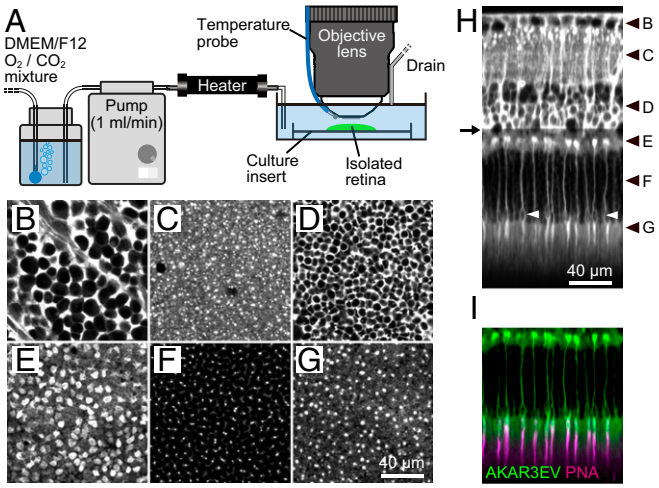

Fig. 1. Two-photon imaging of the PKAchu retina. (*A*) Imaging setup. The isolated PKAchu retina was flat mounted on a culture insert, perfused with DMEM/F12 medium, and imaged using an upright two-photon microscope with a water immersion objective lens. (*B*–*G*) Fluorescent images obtained from the PKAchu retina at the ganglion cell layer (GCL; *B*), inner plexiform layer (IPL; *C*), inner nuclear layer (INL; *D*), outer plexiform layer (OPL; *E*), outer nuclear layer (ONL; *F*), and photoreceptor segments layer (PRS; *G*). Images were obtained by averaging FRET-donor channel (CFP Ch) and FRET-acceptor channel (FRET Ch) images. (*H*) Longitudinal view of the PKAchu retina. The image was reconstructed from z-stack images (214 planes with 1 μm z intervals). White arrowheads indicate cone nuclei. Black arrowheads indicate z positions of the cross-sectional images in *B*–*G*, and an arrow indicates the z position from which the excitation laser power was attenuated to avoid detector saturation. (*I*) Cone labeling with rhodamine labeled peanut agglutinin (PNA-rhodamine) (magenta) overlaid with AKAR3EV signals (green).

stimulation light was delivered onto the retina (*SI Appendix, Supplementary Methods*). Upon a brief 6 s light stimulation, photoreceptors in the dark-adapted retina showed a large drop in PKA activity (Fig. 2 *C* and *D*, dark). Unexpectedly, however, PKA activity rebounded over the basal level, and the increased activity level continued for 30 min. On the other hand, photoreceptors in the light-adapted retina exhibited only a modest suppression of PKA (Fig. 2 *C* and *D*, light) but showed marked PKA activation for 15 min. The suppression was detected within 12 s from the stimulation, and subsequent activation was detected at 50 ± 5 s and peaked at 214 ± 16 s (mean ± SD, $n = 5$; Fig. 2*E*).

In an effort to visualize the light-induced suppression more clearly, we applied a longer 10 min stimulation to the light-adapted retina (Fig. 2 *F* and *G* and Movie S5). In this case, photoreceptor PKA activity exhibited a transient drop in the first 2 min but returned to the basal level for the remaining 8 min. Then, to our surprise, PKA was prominently activated upon light off. We speculate that, upon the light on, the dopamine-mediated PKA suppression occurred and was observed as a transient drop at 2 min. However, simultaneously, an antagonizing light-induced PKA activation occurred with slow kinetics that canceled out the suppression during the subsequent 8 min. Then, upon light off, the dopamine effect was removed instantly probably due to an efficient dopamine clearance from the extrasynaptic space (42), and only the activation remained to shape the apparent off response. Because such light-induced PKA activation has not been reported in normal photoreceptor cells (but see refs 43, 44), hereafter, we focused on this PKA activation using light-adapted retinas.

Light-Off-Induced PKA Activation Occurs Exclusively in Rod Photoreceptor Cells. To determine cell type specificity of the light-off-induced PKA activation, we first examined spatial confinement of the activation in photoreceptor cells. The light spot was projected at the center of the view field (dashed circle in Fig. 3*A*), and time courses of the PKA activation were compared among four areas: three inside and one outside of the light spot (Fig. 3*B*). The activation was sharply confined to the illuminated area (Fig. 3*C*).

We also confirmed that the response was mediated by the phosphorylation on the FRET biosensor AKAR3EV but not by bleaching/switching of its fluorophores. PKAchu-NC mice were used for this purpose. This negative control mouse strain carries AKAR3EV-NC, which has an alanine substitution at the threonine residue in the PKA substrate motif (*SI Appendix*, Fig. S1*C*) (29). In PKAchu-NC retinas, light-induced changes were not observed (Fig. 3 *A* and *C* and Movie S6), confirming that the light

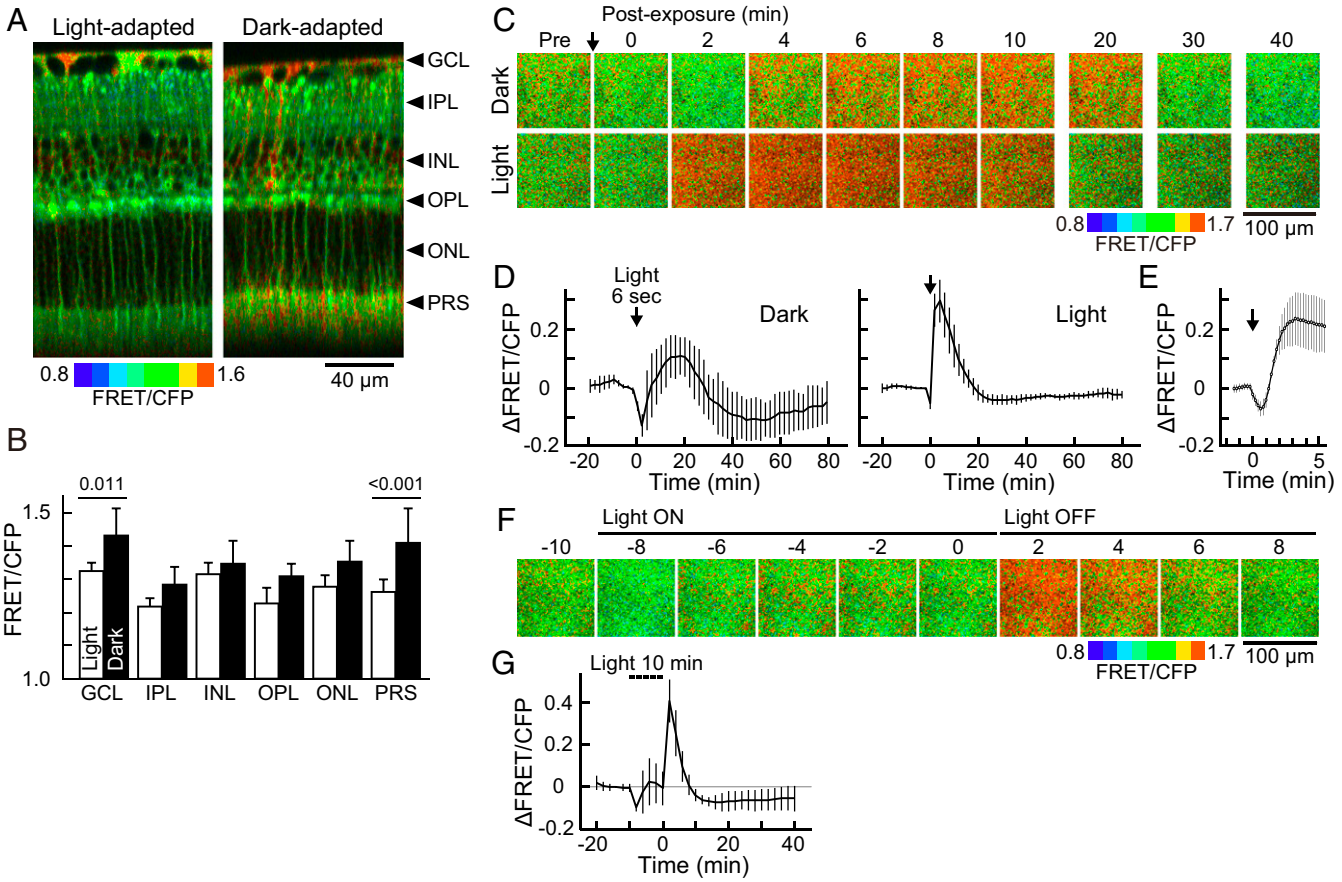

Fig. 2. Basal PKA activities and light-induced PKA activity changes in the dark- and light-adapted PKAchu retinas. (*A*) Longitudinal PKA activity images. Arrowheads indicate the positions of each layer analyzed in *B*. (*B*) FRET/CFP values obtained from each layer of the retina. Mean ± SD, $n = 7$ and 18 measurements for light- and dark-adapted retinas, respectively. The numbers on the bars are *P* values from Tukey–Kramer's test following a two-way ANOVA. (*C*) Time-lapse PKA activity images from dark- and light-adapted retinas. Images are cross-sectional views obtained at the PRS layer. An arrow indicates the timing of a 6 s light stimulation (500 nm and 1.0×10^7 photons μm^{-2} s^{-1}). (*D*) Time courses of the PKA activity at the PRS layer in dark- and light-adapted retinas. Mean ± SD ($n = 3$ and 8 measurements, respectively). (*E*) The early phase of the light response in light-adapted retinas. Mean ± SD ($n = 5$). (*F*) Time-lapse PKA activity images at the PRS layer in the light-adapted retina. Bars indicate the timing of a 10 min light stimulation (500 nm and 3.2×10^7 photons μm^{-2} s^{-1}). (*G*) Time course of the PKA activity at the PRS layer. A dashed bar indicates the timing of light stimulation. Light was temporarily turned off four times for image acquisitions (every 2 min for <10 s each). Mean ± SD ($n = 4$). Data points in *D*, *E* and *F* were obtained every 2 min, 12 s, and 2 min, respectively.

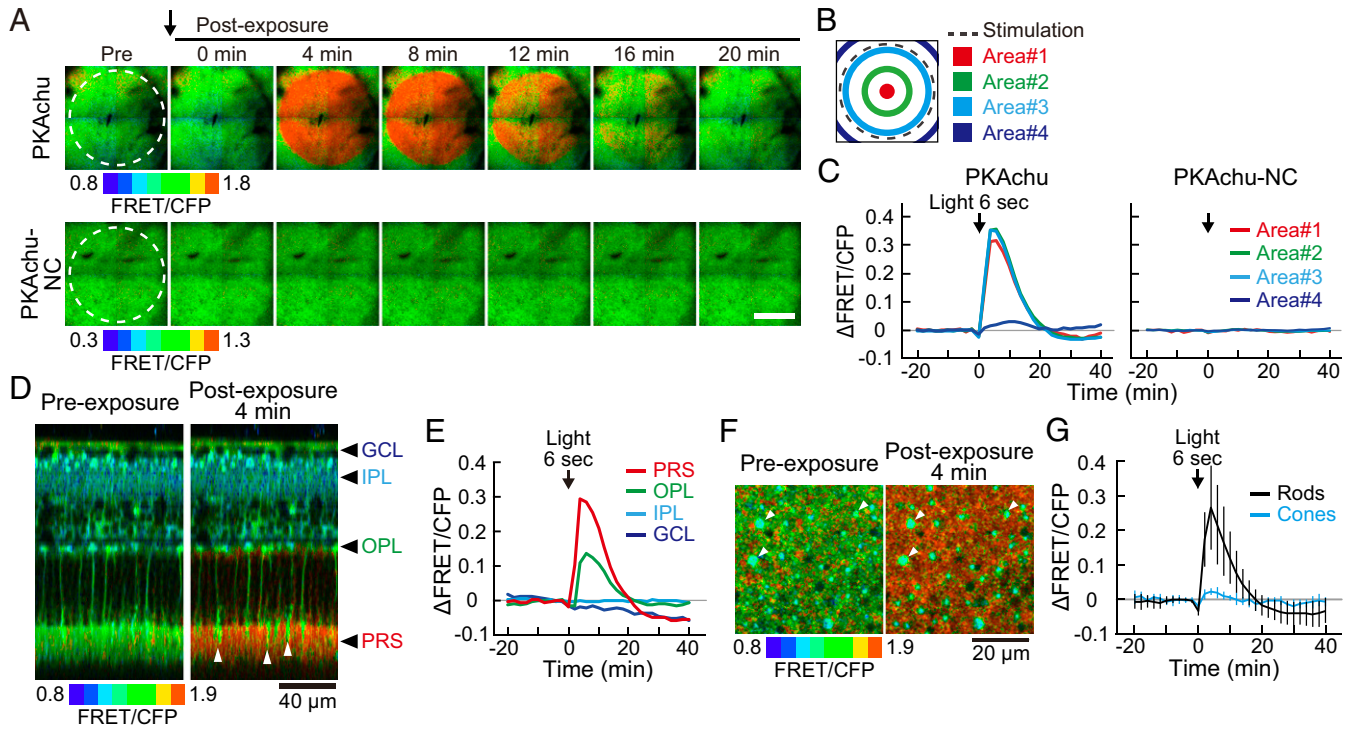

Fig. 3. Spatial distribution of the light-off-induced PKA activation. (*A*) Time-lapse PKA activity images from light-adapted PKAchu and PKAchu-NC retinal explants. Images are cross-sectional views at the PRS layer. Light stimulation (dashed circle, wavelength 500 nm, 1.0×10^8 photons μm^{-2} s^{-1}, and 6 s) was given just before 0 min (arrow). (Scale bar, 400 μm.) (*B*) Positions of four areas analyzed in *C*. (*C*) Time courses of the ΔFRET/CFP in the 6 s stimulation experiments. Values are the means of five (PKAchu) and three (PKAchu-NC) measurements. (*D*) Longitudinal view of the light-induced PKA activation toward 6 s stimulation (500 nm and 1.0×10^8 photons μm^{-2} s^{-1}). Images were reconstructed from a z stack of 61 images with 3 μm z intervals. White arrowheads show cones. Black arrowheads indicate the layer positions analyzed in *E*. (*E*) Time courses of the light-induced PKA activity change at the four indicated layers. Values are the mean of four measurements. (*F*) High-magnification cross-sectional view of the light-off-induced PKA activation at the PRS layer. Images were obtained before and after the 6 s stimulation (500 nm and 1.0×10^8 photons μm^{-2} s^{-1}). White arrowheads indicate cones. (*G*) Time courses of the light-induced PKA activity change in rods (black) and cones (cyan) in the 6 s stimulation experiments. Rod and cone signals were separated by intensity-based image segmentation. Values are the mean ± SD ($n = 8$ measurements). Data points in *C*, *E*, and *G* were obtained every 2 min. An arrow in each panel indicates the timing of light stimulation.

response in the PKAchu retina is induced by the phosphorylation of the AKAR3EV.

Next, to study the cell-type specificity of the PKA activation, we performed five-dimensional imaging (x, y, z, time, and PKA activity). Longitudinal reconstruction images showed that PKA was activated exclusively in photoreceptor cells, especially at PRS (Fig. 3 *D* and *E* and Movie S7). A small number of cells in PRS showed less activation (Fig. 3*D*, arrowheads) than did surrounding cells, suggesting that PKA was activated less efficiently in cones than in rods. Indeed, rod-specific PKA activation was visualized in high-magnification cross-sectional images (Fig. 3 *F* and *G* and Movie S8). Taken together, these results indicated that the light-off-induced PKA activation occurs exclusively in light-exposed rod photoreceptor cells. In the following experiments, we further characterized this PKA activation in rods.

Light-Induced PKA Activation Is Driven by Rhodopsin and Transducin. To identify the photopigment that drives the light-off-induced PKA activation, we analyzed the spectral sensitivity of the response. For this purpose, responses toward various intensities of light were recorded from rods (*SI Appendix*, Fig. S3*A*). Measurements were performed for seven different wavelengths to obtain a series of intensity-response relationships (*SI Appendix*, Fig. S3*B*). Then, half-saturating light intensities ($I_{1/2}$) were estimated by fitting. The inverse of $I_{1/2}$ values were plotted as a function of wavelength to obtain the spectral sensitivity (Fig. 4*A*). Assuming that the light-induced PKA activation would be triggered by an opsin-family photopigment, the data were fitted with an A1-pigment spectral template (45). The estimated λ_{max} was 489 nm, which suggests the involvement of rhodopsin (500 nm), isorhodopsin (487 nm) (46), and M-cone pigment (508 nm) in the PKA activation. Intriguingly, the estimated maximum amplitude increased as the wavelength became longer (*SI Appendix*, Fig. S3*C*), which is opposite to the activity regulation of melanopsin (see *Discussion* for details).

To validate the involvement of rhodopsin in the light-off-induced PKA activation, we crossed PKAchu mice with *Gnat1*$^{-/-}$ mice, which lack the α subunit of the G protein transducin and are deficient in rhodopsin-mediated signal transduction in rods (47). The amplitude of the response in PRS was clearly decreased in PKAchu *Gnat1*$^{+/-}$ and completely lost in PKAchu *Gnat1*$^{-/-}$ (Fig. 4*B*), showing the critical roles of rhodopsin and transducin in the light-off-induced PKA activation. Notably, the estimated half-saturating light intensity for 500 nm light was 6.5×10^7 photons μm^{-2} (*SI Appendix*, Fig. S3*B*), which is $>10^4$-fold greater than that of the visual photoresponse in rods (48). In such a high intensity range, the normal rod phototransduction is completely saturated. Thus, these data suggest the presence of an alternative rod phototransduction mechanism, which is activated exclusively with intense illumination.

Both Rhodopsin and Isorhodopsin Were Detected in Our Light-Adapted Retinal Explant. The estimated λ_{max} of the light-off-induced PKA photoresponse (489 nm) was 11 nm shorter than the absorption

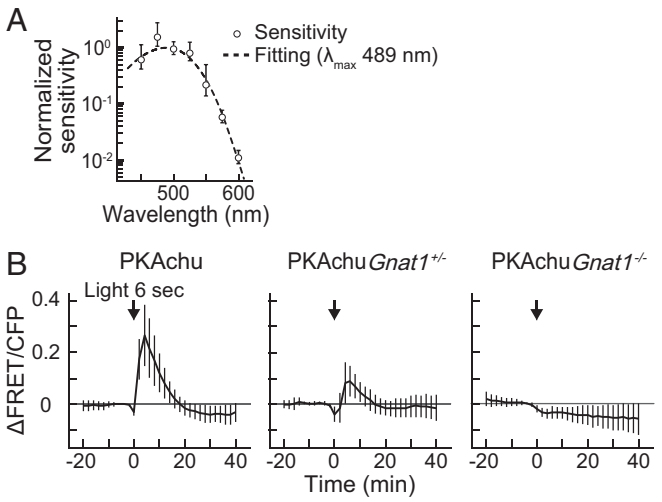

Fig. 4. Involvement of rhodopsin and transducin in the light-off-induced PKA activation. (*A*) Spectral sensitivity plot of the light-induced rod PKA activation. Plots were fitted with the spectral template of the visual pigment to obtain the estimated λ_{max} of 489 nm (dashed curve). Data were normalized to the peak of the curve. Values are the mean ± SEM (n = 3–7). (*B*) Time courses of the PKA activity in the 6 s stimulation experiments, obtained from rods imaged at PRS in wild-type PKAchu, PKAchu *Gnat1*$^{+/-}$, and PKAchu *Gnat1*$^{-/-}$. Data for wild-type PKAchu is a replot of Fig. 3*G*. An arrow in each panel indicates the timing of 6 s light stimulation (500 nm and 1×10^8 photons μm^{-2}). Values are the mean ± SD (n = 9 for PKAchu *Gnat1*$^{+/-}$ and n = 18 for PKAchu *Gnat1*$^{-/-}$).

maximum of rhodopsin (500 nm). To study the cause of this blueshift, we analyzed the absorption spectrum of photopigment extracted from our light-adapted retinal explant. Wild-type C57BL6/J (B6J) retinas were flat mounted using the protocol performed in the PKA activity imaging, then, solubilized for absorption measurements. As a control, retinas from dark-adapted mice were collected under dim red light. Absorption of photopigment was detected from both light- and dark-adapted retinas at around 500 nm (Fig. 5*A*). The peak height of the light-adapted sample was 16 ± 1% (mean ± SD, n = 3) of the height observed for the dark-adapted control. Surprisingly, the absorption maximum of the light-adapted preparation was detected at 495 ± 2 nm (mean ± SD, n = 3; Fig. 5*B*, Light), which was 7 nm shorter than that of the dark-adapted control (504 ± 1 nm; Fig. 5*B*, Dark) and well fitted with the spectral sensitivity plot of the light-off-induced PKA activation (Fig. 5*C*).

We speculated that the blueshifted absorbance was caused by the formation of isorhodopsin, which contains a 9-*cis* retinal and shows an absorption maximum at 487 nm (46). Indeed, the obtained absorption spectrum was fitted well with the sum of the rhodopsin and isorhodopsin templates (Fig. 5*D*). To verify the presence of isorhodopsin, the chromophore composition was determined by normal phase high performance liquid chromatography (HPLC; Fig. 5*E*). Most of the 11-*cis* retinal, which comprises 90 ± 3% (mean ± SD, n = 2) of total retinoids in the dark-adapted control (Fig. 5 *E* and *F*, Dark), was converted to all-*trans* retinal and all-*trans* retinol in the light-adapted sample (Fig. 5 *E* and *F*, Light). In agreement with the absorbance data, the 11-*cis* retinal and 9-*cis* retinal were also detected at comparable levels: 9.0 ± 2.3% and 8.3 ± 0.8%, respectively (mean ± SD, n = 3; Fig. 5 *E* and *F*, Light). Therefore, we concluded that isorhodopsin is formed specifically in the light-adapted retinal explants and produces the blueshifted spectral sensitivity of the light-off-induced PKA activation.

Rhodopsin-Deficient Albino PKAchu Rods Show Only the Light-On-Induced PKA Suppression. To further investigate the involvement of rhodopsin, we used albino mice, which show a greater reduction in rhodopsin level compared to their wild-type counterparts when kept under bright light (49). Although, rhodopsin content in the dark-adapted albino retina was 51 ± 5% (mean ± SD, n = 4) to the wild-type level, surprisingly, that of the light-adapted albino retina was less than the detection limit (Fig. 6*A*, Albino), without any thinning in the ONL thickness (53.9 ± 1.3 μm at 1 mm superior from the ONH; mean ± SD, n = 6 retinas). The albino retina exhibited markedly higher basal PKA activity in the PRS layer than the wild type (Fig. 6 *B* and *C*). This high basal PKA activity in PRS was suppressed to nearly the wild-type level in the presence of 100 nM exogenous dopamine (Fig. 6*D*), suggesting a decreased dopamine level in the albino retina. In fact, the albino mice used in this study (B6N-Tyr$^{c\text{-}Brd}$/BrdCrCrl; B6 albino) are deficient in tyrosinase, which supports dopamine biogenesis (50).

We performed the photostimulation experiments with albino PKAchu retinas. In stark contrast to the wild type, only transient suppression was observed following a brief 6 s stimulation (Fig. 6*E*, Albino). Moreover, the PKA activity was kept at a low

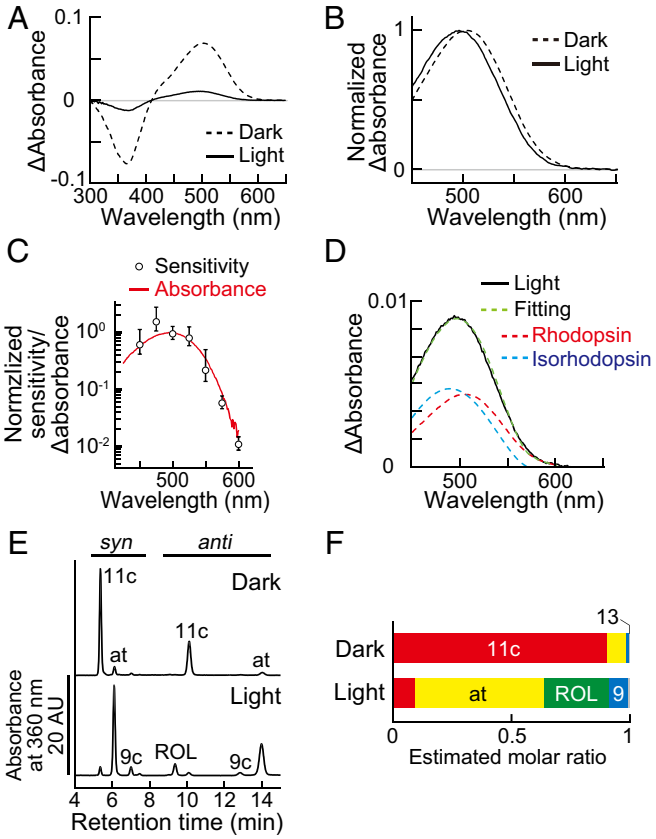

Fig. 5. Formation of isorhodopsin in the light-adapted retinal explant. (*A*) Difference absorption spectra of retinal photopigments measured at 4 °C. Solid curve: light-adapted retinal explants and dashed curve: dark-adapted control. Values are the average of three measurements. Each sample was prepared from one retina. (*B*) Normalized spectra created from the data in *A*. (*C*) A comparison between the difference absorption spectrum of the light-adapted retina (red) and the spectral sensitivity data (open circles, replot of Fig. 4*A*). Note that the vertical axis is in logarithmic scale. (*D*) Data fitting with rhodopsin (red) and isorhodopsin templates (cyan). The averaged spectrum of the light-adapted retina (solid black curve, replot from [*A*]) was fitted with the sum of the rhodopsin and isorhodopsin spectra (green). (*E*) HPLC chromatogram of retinoids extracted from a dark- or light-adapted retina. Retinal isomers were extracted as *syn*- and *anti*-oxime forms, separated by the normal phase HPLC, and detected by their absorbance at 360 nm. (*F*) Molar ratio of the retinoids estimated by HPLC. Values are the means of two and three measurements for dark- and light-adapted retinas, respectively. The 11c: 11-*cis* retinal; at: all-*trans* retinal; 9c: 9-*cis* retinal; 13: 13-*cis* retinal; ROL: all-*trans* retinol.

level during a 10 min stimulation and returned to the basal level upon light off without a prominent overshoot (Fig. 6*F* and Movie S9). These data further support the notion that rhodopsin plays a critical role in the light-off-induced PKA activation in rods.

Discussion

In the present study, we report a two-photon live imaging method to visualize PKA activity in all layers of the retina (Fig. 1, *SI Appendix*, Fig. S2, and Movies S1–S4) and describe the light-off-induced PKA activation in rods (Fig. 3 and Movies S7 and S8). The light-on-induced reduction of retinal cAMP was reported in previous studies (16, 41, 51). Here, our live imaging approach with high spatiotemporal resolution has succeeded in characterizing the light-off-induced PKA activation. Application of two-photon microscopy to the retina is technically difficult because visual pigments are substantially activated by both high-power infrared excitation laser and fluorescence emission from probes, which cause a low-photopic level of activation in the visual transduction system (52) (*SI Appendix*). The light-off-induced PKA activation was readily observed, probably because this response requires a high-photopic level of illumination from the external light source (*SI Appendix*, Figs. S3 and S4).

The mechanism underlying the light-off-induced PKA activation is still unknown, but we suggest that this mechanism likely involves two different light-dependent pathways: a PKA suppression pathway with fast kinetics and a PKA activation pathway with slow kinetics (Fig. 6*G*). Rhodopsin-containing wild-type PKAchu retinas showed transient PKA suppression during the 10 min light-on period followed by immediate and robust PKA activation upon light off (Fig. 6*F* and Movie S9). In contrast, the albino PKAchu explants showed persistent PKA suppression during the 10 min light-on period (Fig. 6*F* and Movie S9). Because rhodopsin was not detected in the albino retinal explant (Fig. 6*A*), this persistent suppression is likely to be mediated by the light-induced dopamine release that can be triggered by cone visual pigments and/or melanopsin in intrinsically photosensitive retinal ganglion cells (15) (but see ref. 14). We speculate that the persistent PKA suppression also operates in wild-type mice during the light-on period, but that its presence is masked by rhodopsin-mediated PKA activation. The fast kinetics of the suppression pathway is supported by the observation that the PKA activity is restored immediately after light off in the albino PKAchu (Fig. 6*F*).

Rhodopsin and transducin play critical roles in the light-off-induced PKA activation (Fig. 4). Isorhodopsin is detected in the retina (Fig. 5*E*) but is not necessarily required for the light-off-induced PKA activation because the response was also observed in dark-adapted PKAchu retinas devoid of the 9-*cis* retinal (Figs. 2*C* and 5*F*). Conventional phototransduction, which utilizes the cGMP system (1–3), is also not likely to underlie the mechanism by the two reasons. First, the working light intensity of the light-off-induced PKA activation (*SI Appendix*, Fig. S3 *A* and *B*) is $>10^4$-fold higher than that of the rod visual transduction (48). Second, the duration of the light-off-induced PKA activation is >10 min (Fig. 3); this is clearly longer than that of the visual photoresponse, which ends in a few seconds (48). Therefore, we speculate the presence of an alternative pathway acting downstream of transducin. Because the light-off-induced PKA activation is strictly confined within the illuminated region (Fig. 3 *A*–*C* and Movie S6), intercellular signaling mechanisms may be excluded from this process.

One possible mechanism underlying the transducin-mediated PKA activation is the light-dependent transducin translocation. The Ca^{2+}-insensitive AC isoforms are enriched in the photoreceptor inner segment (53). It is suggested that transducin stimulates AC in primary culture of tiger salamander rods (43). Rod transducin is localized in the outer segment in darkness but moves to the inner segment under bright light. This translocation contributes to the rod survival and synaptic transmission to rod bipolar cells (54) and is suggested to be a mechanism to escape from rod saturation (55). The transducin translocation occurs under the light level that saturates rod photoresponse with a half-time of completion of 5 and 12.5 min for α and β subunits, respectively (56, 57). These features

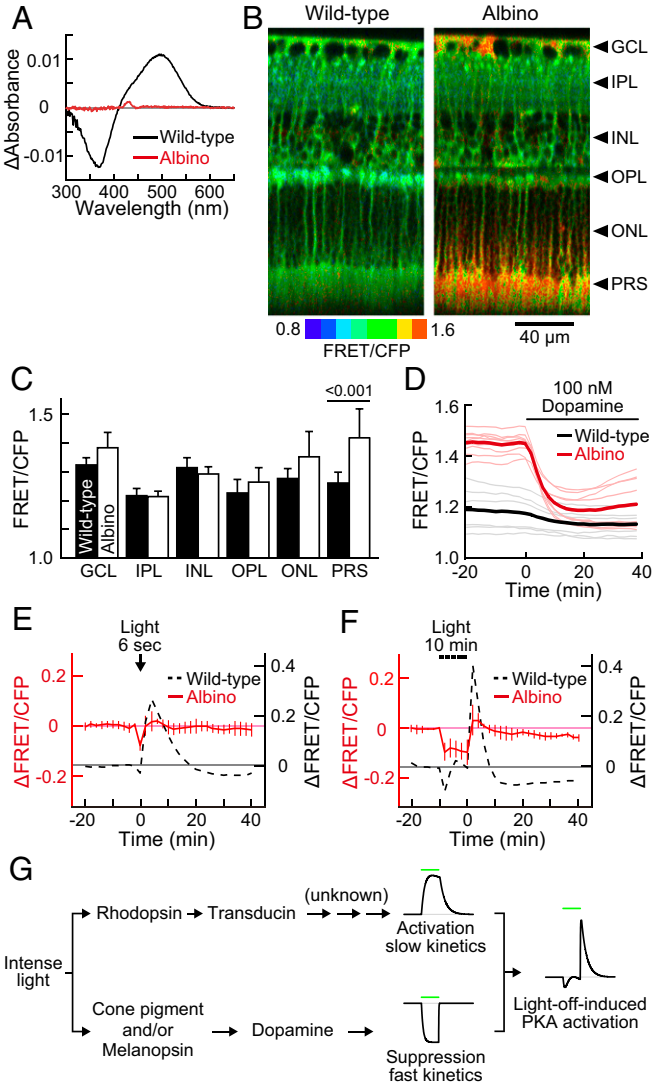

Fig. 6. Basal PKA activity and light-induced PKA suppression in the albino PKAchu retina. (*A*) Difference absorption spectra of membrane proteins extracted from a wild-type (black) or an albino (red) mouse retina. Values are the means of three samples. (*B*) Longitudinal PKA activity images of wild-type and albino PKAchu retinas. Arrowheads indicate the positions of each layer analyzed in *C*. (*C*) FRET/CFP values obtained from each layer of the retina. Mean ± SD, $n = 7$ and 14 measurements for the wild-type and albino retinas, respectively. The number on the bar is a *P* value from Tukey–Kramer's test following a two-way ANOVA. (*D*) Responses of rod PKA to 100 nM dopamine perfusion in wild-type (black) and albino (red) PKAchu retinas. Light-colored thin curves and dark-colored bold curves are individual and averaged data, respectively. (*E* and *F*) Light-induced PKA activity changes in response to 6 s stimulation (*E*; 500 nm and 1.0×10^8 photons μm^{-2} s^{-1}) and 10 min stimulation (*F*; 500 nm and 3.2×10^7 photons μm^{-2} s^{-1}). Albino data (red, mean ± SD, $n = 4$ and 5, respectively) are adjusted 0.16 upward from the wild-type data (dashed black) with consideration for the average difference in the basal FRET/CFP (PRS in *C*). Wild-type data are replots of Figs. 3*G* and 2*G*, respectively. Data points were obtained every 2 min. (*G*) A hypothetical model of the light-off-induced PKA activation. Green bars show the timing of a light stimulation.

coincide with the high half-saturation light intensity (*SI Appendix*, Fig. S3) and time course (Fig. 2) of the light-off-induced PKA activation. In addition, cone transducin does not show the translocation (58), in line with the lack of the light-off-induced PKA activation in cones (Fig. 3*F*). Interestingly, phosphorylation of phosducin, one of the PKA targets in rods (21), facilitates the recovery from the translocation (59). The transducin-mediated PKA activation may constitute a feedback loop to transducin for the recovery from the translocation to boost the dark adaptation.

The presence of isorhodopsin in our light-adapted retinal explants was unexpected (Fig. 5). As a similar example, photoregeneration of isorhodopsin was reported previously in frog retinal explants (60). In that case, the isorhodopsin was thought to be a product of back photoconversion from a Meta-III intermediate of rhodopsin. It is tempting to speculate that low-quantum yield isorhodopsin (61) plays a role in rod light adaptation. However, we suppose that isorhodopsin is not formed in the mouse retina in vivo because the 9-*cis* retinal is not detected from retinoids directly extracted from light-adapted mouse eyes (62). We speculate that isorhodopsin formation is an artifact caused by our sample preparation in which retinas were temporarily exposed to light at room temperature.

The maximum amplitude of the light-off-induced PKA activation became larger as the light stimulus was shifted to longer wavelengths (*SI Appendix*, Fig. S3 *B* and *C*). As the spectral sensitivity showed its maxima at 489 nm (Fig. 4*A*), this discrepancy suggests the input from another photopigment(s) that independently regulates the amplitude. Melanopsin displays a tristable photoequilibrium, and the fraction of its signaling form is decreased as the wavelength becomes longer within the 400–600 nm range (63, 64). Therefore, we speculate that red light-induced melanopsin inactivation increases the amplitude of the light-off-induced PKA activation via the aforementioned dopamine-mediated pathway.

Lastly, what is the physiological role of the light-off-induced PKA activation? Previous biochemical studies have shown that PKA phosphorylates many phototransduction components (19–22) and the gap junction protein (24). Electrophysiological studies have shown that cAMP improves the rod photosensitivity (11, 23). Taken together, these findings suggest that PKA promotes the dark adaptation of rods. In support of this notion, recent studies by Kolesnikov and colleagues reported a delayed rod dark adaptation in mutant mice whose GRK1 is mutated to block its cAMP-dependent phosphorylation (65). PKA phosphorylates GRK1 to reduce its rhodopsin phosphorylation ability (19), which, in turn, extends the active lifetime of rhodopsin to increase the photosensitivity. They also reported lack of phenotype in cone dark adaptation, which is consistent with the lack of responses in our PKAchu cones (Fig. 3 *F* and *G*). Therefore, we speculate that the physiological role of the light-off-induced PKA activation is the acceleration of rod dark adaptation upon the transition from a light to a dark environment. Further physiological studies will be needed to quantitatively describe the contribution of PKA in rod dark adaptation.

Materials and Methods

Animals. The animal protocols were reviewed and approved by the Animal Care and Use Committee of Kyoto University Graduate School of Medicine (MedKyo17539, 17539-2, 18086, 19090, and 20081). Colonies of wild-type PKAchu (nbio185; NIBIOHN) and PKAchu-NC (nbio186) transgenic mouse lines were maintained in a heterozygous state on the B6J background. Albino PKAchu was obtained by crossing with B6 albino (Charles River Laboratories Japan). PKAchu Gnat1$^{+/-}$ and PKAchu Gnat1$^{-/-}$ were obtained by crossing wild-type PKAchu with Gnat1$^{-/-}$ (B6J background; the kind gift from Vladimir J. Kefalov, Washington University in St. Louis, St. Louis, MO) for two to three generations.

Two-Photon Live Imaging of the Retinal Explant. A flat-mounted retina was perfused with oxygenated medium and imaged with an upright multiphoton microscope system (Fluoview FV1000MPE; Olympus) using a water immersion objective lens (XLPLN25XWMP; Olympus). Stimulation light was generated with a custom-made light-emitting diode system (*SI Appendix*, Fig. S4) and delivered to the retina through the objective lens.

All additional experimental details are provided in *SI Appendix*, Supplementary Methods.

Data Availability. All study data are included in the article and supporting information.

ACKNOWLEDGMENTS. Support was received in the form of the following: Japan Society for the Promotion of Science, Grant-in-Aid for Scientific Research (JSPS KAKENHI; 15H05949 "Resonance Bio" to M.M., 16H06280 "ABiS" to M.M., 19H00993 to M.M.; and 19K16087 to S.S.); Japan Science and Technology Agency, Core Research for Evolutional Science and Technology (JST CREST) "OptoBio" (JPMJCR1654 to M.M. and JPMJCR1753 to T.Y.); Japan Agency for Medical Research and Development (AMED; 19gm5010003h0003 to M.M.); The Shimizu Foundation for Immunology and Neuroscience Grant for 2017 (S.S.); The Kyoto University Research Fund for Young Scientists (Start-up) FY2017 (S.S.); The Kyoto University Foundation (S.S.). The authors acknowledge the technical assistance of the machine shop in Kyoto University. The authors thank Dr. Vladimir J. Kefalov (Washington University in St. Louis) for providing *Gnat1*$^{-/-}$ mice and for his helpful discussions and comments on the paper.

1. S. Kawamura, S. Tachibanaki, Rod and cone photoreceptors: Molecular basis of the difference in their physiology. *Comp. Biochem. Physiol. A Mol. Integr. Physiol.* **150**, 369–377 (2008).
2. G. L. Fain, R. Hardie, S. B. Laughlin, Phototransduction and the evolution of photoreceptors. *Curr. Biol.* **20**, R114–R124 (2010).
3. T. D. Lamb, Evolution of phototransduction, vertebrate photoreceptors and retina. *Prog. Retin. Eye Res.* **36**, 52–119 (2013).
4. K. W. Yau, R. C. Hardie, Phototransduction motifs and variations. *Cell* **139**, 246–264 (2009).
5. L. Astakhova, M. Firsov, V. Govardovskii, Activation and quenching of the phototransduction cascade in retinal cones as inferred from electrophysiology and mathematical modeling. *Mol. Vis.* **21**, 244–263 (2015).
6. X. H. Wen, A. M. Dizhoor, C. L. Makino, Membrane guanylyl cyclase complexes shape the photoresponses of retinal rods and cones. *Front. Mol. Neurosci.* **7**, 45 (2014).
7. O. P. Gross, E. N. Pugh Jr., M. E. Burns, cGMP in mouse rods: the spatiotemporal dynamics underlying single photon responses. *Front. Mol. Neurosci.* **8**, 6 (2015).
8. F. Vinberg, J. Chen, V. J. Kefalov, Regulation of calcium homeostasis in the outer segments of rod and cone photoreceptors. *Prog. Retin. Eye Res.* **67**, 87–101 (2018).
9. J. Zang, S. C. F. Neuhauss, The binding properties and physiological functions of recoverin. *Front. Mol. Neurosci.* **11**, 473 (2018).
10. I. I. Senin II, K. W. Koch, M. Akhtar, P. P. Philippov, Ca2+-dependent control of rhodopsin phosphorylation: Recoverin and rhodopsin kinase. *Adv. Exp. Med. Biol.* **514**, 69–99 (2002).
11. L. A. Astakhova, D. A. Nikolaeva, T. V. Fedotkina, V. I. Govardovskii, M. L. Firsov, Elevated cAMP improves signal-to-noise ratio in amphibian rod photoreceptors. *J. Gen. Physiol.* **149**, 689–701 (2017).
12. E. Popova, Role of dopamine in distal retina. *J. Comp. Physiol. A Neuroethol. Sens. Neural Behav. Physiol.* **200**, 333–358 (2014).
13. P. Witkovsky, Dopamine and retinal function. *Doc. Ophthalmol.* **108**, 17–40 (2004).
14. V. Pérez-Fernández *et al.*, Rod photoreceptor activation alone defines the release of dopamine in the retina. *Curr. Biol.* **29**, 763–774.e5 (2019).
15. C. L. Prigge *et al.*, M1 ipRGCs influence visual function through retrograde signaling in the retina. *J. Neurosci.* **36**, 7184–7197 (2016).
16. A. I. Cohen, R. D. Todd, S. Harmon, K. L. O'Malley, Photoreceptors of mouse retinas possess D4 receptors coupled to adenylate cyclase. *Proc. Natl. Acad. Sci. U.S.A.* **89**, 12093–12097 (1992).
17. C. R. Jackson, S. S. Chaurasia, C. K. Hwang, P. M. Iuvone, Dopamine D_4 receptor activation controls circadian timing of the adenylyl cyclase 1/cyclic AMP signaling system in mouse retina. *Eur. J. Neurosci.* **34**, 57–64 (2011).
18. K. A. Neve, J. K. Seamans, H. Trantham-Davidson, Dopamine receptor signaling. *J. Recept. Signal Transduct. Res.* **24**, 165–205 (2004).
19. T. J. Horner, S. Osawa, M. D. Schaller, E. R. Weiss, Phosphorylation of GRK1 and GRK7 by cAMP-dependent protein kinase attenuates their enzymatic activities. *J. Biol. Chem.* **280**, 28241–28250 (2005).
20. N. Balasubramanian, K. Levay, T. Keren-Raifman, E. Faurobert, V. Z. Slepak, Phosphorylation of the regulator of G protein signaling RGS9-1 by protein kinase A is a potential mechanism of light- and Ca2+-mediated regulation of G protein function in photoreceptors. *Biochemistry* **40**, 12619–12627 (2001).
21. H. Song, M. Belcastro, E. J. Young, M. Sokolov, Compartment-specific phosphorylation of phosducin in rods underlies adaptation to various levels of illumination. *J. Biol. Chem.* **282**, 23613–23621 (2007).

22. G. Wolbring, P. P. Schnetkamp, Modulation of the calcium sensitivity of bovine retinal rod outer segment guanylyl cyclase by sodium ions and protein kinase A. *Biochemistry* **35**, 11013–11018 (1996).
23. L. A. Astakhova, E. V. Samoiliuk, V. I. Govardovskii, M. L. Firsov, cAMP controls rod photoreceptor sensitivity via multiple targets in the phototransduction cascade. *J. Gen. Physiol.* **140**, 421–433 (2012).
24. H. Li *et al*., Adenosine and dopamine receptors coregulate photoreceptor coupling via gap junction phosphorylation in mouse retina. *J. Neurosci.* **33**, 3135–3150 (2013).
25. P. H. Li, J. Verweij, J. H. Long, J. L. Schnapf, Gap-junctional coupling of mammalian rod photoreceptors and its effect on visual detection. *J. Neurosci.* **32**, 3552–3562 (2012).
26. A. Goto *et al*., Circuit-dependent striatal PKA and ERK signaling underlies rapid behavioral shift in mating reaction of male mice. *Proc. Natl. Acad. Sci. U.S.A.* **112**, 6718–6723 (2015).
27. T. Yamaguchi *et al*., Role of PKA signaling in D2 receptor-expressing neurons in the core of the nucleus accumbens in aversive learning. *Proc. Natl. Acad. Sci. U.S.A.* **112**, 11383–11388 (2015).
28. R. Mizuno *et al*., In vivo imaging reveals PKA regulation of ERK activity during neutrophil recruitment to inflamed intestines. *J. Exp. Med.* **211**, 1123–1136 (2014).
29. Y. Kamioka *et al*., Live imaging of protein kinase activities in transgenic mice expressing FRET biosensors. *Cell Struct. Funct.* **37**, 65–73 (2012).
30. N. Komatsu *et al*., Development of an optimized backbone of FRET biosensors for kinases and GTPases. *Mol. Biol. Cell* **22**, 4647–4656 (2011).
31. M. A. Samuel, Y. Zhang, M. Meister, J. R. Sanes, Age-related alterations in neurons of the mouse retina. *J. Neurosci.* **31**, 16033–16044 (2011).
32. C. Behrens, T. Schubert, S. Haverkamp, T. Euler, P. Berens, Connectivity map of bipolar cells and photoreceptors in the mouse retina. *eLife* **5**, e20041 (2016).
33. L. V. Johnson, G. S. Hageman, J. C. Blanks, Interphotoreceptor matrix domains ensheath vertebrate cone photoreceptor cells. *Invest. Ophthalmol. Vis. Sci.* **27**, 129–135 (1986).
34. J. Zhang, Y. Ma, S. S. Taylor, R. Y. Tsien, Genetically encoded reporters of protein kinase A activity reveal impact of substrate tethering. *Proc. Natl. Acad. Sci. U.S.A.* **98**, 14997–15002 (2001).
35. K. Aoki, M. Matsuda, Visualization of small GTPase activity with fluorescence resonance energy transfer-based biosensors. *Nat. Protoc.* **4**, 1623–1631 (2009).
36. D. Mustafi *et al*., Transcriptome analysis reveals rod/cone photoreceptor specific signatures across mammalian retinas. *Hum. Mol. Genet.* **25**, 4376–4388 (2016).
37. D. G. McMahon, P. M. Iuvone, G. Tosini, Circadian organization of the mammalian retina: From gene regulation to physiology and diseases. *Prog. Retin. Eye Res.* **39**, 58–76 (2014).
38. P. Farshi, B. Fyk-Kolodziej, D. M. Krolewski, P. D. Walker, T. Ichinose, Dopamine D1 receptor expression is bipolar cell type-specific in the mouse retina. *J. Comp. Neurol.* **524**, 2059–2079 (2016).
39. A. I. Cohen, C. Blazynski, Dopamine and its agonists reduce a light-sensitive pool of cyclic AMP in mouse photoreceptors. *Vis. Neurosci.* **4**, 43–52 (1990).
40. I. Nir *et al*., Dysfunctional light-evoked regulation of cAMP in photoreceptors and abnormal retinal adaptation in mice lacking dopamine D4 receptors. *J. Neurosci.* **22**, 2063–2073 (2002).
41. C. R. Jackson *et al*., Essential roles of dopamine D4 receptors and the type 1 adenylyl cyclase in photic control of cyclic AMP in photoreceptor cells. *J. Neurochem.* **109**, 148–157 (2009).
42. Z. Cheng, Y. M. Zhong, X. L. Yang, Expression of the dopamine transporter in rat and bullfrog retinas. *Neuroreport* **17**, 773–777 (2006).
43. P. D. Alfinito, E. Townes-Anderson, Activation of mislocalized opsin kills rod cells: A novel mechanism for rod cell death in retinal disease. *Proc. Natl. Acad. Sci. U.S.A.* **99**, 5655–5660 (2002).
44. J. Wang, N. Zhang, A. Beuve, E. Townes-Anderson, Mislocalized opsin and cAMP signaling: A mechanism for sprouting by rod cells in retinal degeneration. *Invest. Ophthalmol. Vis. Sci.* **53**, 6355–6369 (2012).
45. V. I. Govardovskii, N. Fyhrquist, T. Reuter, D. G. Kuzmin, K. Donner, In search of the visual pigment template. *Vis. Neurosci.* **17**, 509–528 (2000).
46. J. Fan, B. Rohrer, G. Moiseyev, J. X. Ma, R. K. Crouch, Isorhodopsin rather than rhodopsin mediates rod function in RPE65 knock-out mice. *Proc. Natl. Acad. Sci. U.S.A.* **100**, 13662–13667 (2003).
47. P. D. Calvert *et al*., Phototransduction in transgenic mice after targeted deletion of the rod transducin alpha -subunit. *Proc. Natl. Acad. Sci. U.S.A.* **97**, 13913–13918 (2000).
48. S. Nymark, R. Frederiksen, M. L. Woodruff, M. C. Cornwall, G. L. Fain, Bleaching of mouse rods: Microspectrophotometry and suction-electrode recording. *J. Physiol.* **590**, 2353–2364 (2012).
49. G. H. Daly, J. M. DiLeonardo, N. R. Balkema, G. W. Balkema, The relationship between ambient lighting conditions, absolute dark-adapted thresholds, and rhodopsin in black and hypopigmented mice. *Vis. Neurosci.* **21**, 925–934 (2004).
50. A. T. Slominski *et al*., "Sensing the environment: Regulation of local and global homeostasis by the skin's neuroendocrine system" in *Advances in Anatomy, Embryology and Cell Biology*, P. Sutovsky, Ed. (Springer, 2012), vol. 212, chap. 2, pp. 7–26.
51. G. W. DeVries, A. I. Cohen, I. A. Hall, J. A. Ferrendelli, Cyclic nucleotide levels in normal and biologically fractionated mouse retina: Effects of light and dark adaptation. *J. Neurochem.* **31**, 1345–1351 (1978).
52. T. Euler, K. Franke, T. Baden, "Studying a light sensor with light: Multiphoton imaging in the retina" in *Multiphoton Microscopy*, E. Hartveit, Ed. (Humana Press, 2019), vol. 148, chap. 10, pp. 225–250.
53. R. M. Abdel-Majid, F. Tremblay, W. H. Baldridge, Localization of adenylyl cyclase proteins in the rodent retina. *Brain Res. Mol. Brain Res.* **101**, 62–70 (2002).
54. A. Majumder *et al*., Transducin translocation contributes to rod survival and enhances synaptic transmission from rods to rod bipolar cells. *Proc. Natl. Acad. Sci. U.S.A.* **110**, 12468–12473 (2013).
55. A. Tikidji-Hamburyan *et al*., Rods progressively escape saturation to drive visual responses in daylight conditions. *Nat. Commun.* **8**, 1813 (2017).
56. E. S. Lobanova *et al*., Transducin translocation in rods is triggered by saturation of the GTPase-activating complex. *J. Neurosci.* **27**, 1151–1160 (2007).
57. M. Sokolov *et al*., Massive light-driven translocation of transducin between the two major compartments of rod cells: A novel mechanism of light adaptation. *Neuron* **34**, 95–106 (2002).
58. E. S. Lobanova *et al*., Mechanistic basis for the failure of cone transducin to translocate: Why cones are never blinded by light. *J. Neurosci.* **30**, 6815–6824 (2010).
59. M. Belcastro *et al*., Phosphorylation of phosducin accelerates rod recovery from transducin translocation. *Invest. Ophthalmol. Vis. Sci.* **53**, 3084–3091 (2012).
60. T. Reuter, Photoregeneration of rhodopsin and isorhodopsin from metarhodopsin III in the frog retina. *Vision Res.* **16**, 909–917 (1976).
61. R. Hubbard, A. Kropf, The action of light on rhodopsin. *Proc. Natl. Acad. Sci. U.S.A.* **44**, 130–139 (1958).
62. K. A. Lee, M. Nawrot, G. G. Garwin, J. C. Saari, J. B. Hurley, Relationships among visual cycle retinoids, rhodopsin phosphorylation, and phototransduction in mouse eyes during light and dark adaptation. *Biochemistry* **49**, 2454–2463 (2010).
63. T. Matsuyama, T. Yamashita, Y. Imamoto, Y. Shichida, Photochemical properties of mammalian melanopsin. *Biochemistry* **51**, 5454–5462 (2012).
64. A. J. Emanuel, M. T. Do, Melanopsin tristability for sustained and broadband phototransduction. *Neuron* **85**, 1043–1055 (2015).
65. A. V. Kolesnikov, J. D. Chrispell, S. Osawa, V. J. Kefalov, E. R. Weiss, Phosphorylation at Serine 21 in G protein-coupled receptor kinase 1 (GRK1) is required for normal kinetics of dark adaption in rod but not cone photoreceptors. *FASEB J.* **34**, 2677–2690 (2020).